Grain Refinement of Aluminum Weld Metal

Titanium and zirconium microadditions have a strong influence on grain size, solidification rate and nucleation time

BY H. YUNJIA, R. H. FROST, D. L. OLSON AND G. R. EDWARDS

ABSTRACT. The influence of titanium and zirconium microadditions on the grain refinement in aluminum weld metal was investigated. These grain refiners significantly altered the morphology of the solidification structure. The time to nucleate the first grain in the weld metal, the weld metal solidification rate and the columnar grain size were all characterized as a function of the grain refiner content. Increasing the zirconium and titanium contents altered the weld pool shape, which increased the solidification rates, increased the nucleation rate and promoted grain refinement. A grain refinement model based on heterogeneous nucleation on second-phase particles is introduced.

Introduction

The formation of aluminum alloy weld metal macrostructures has been studied from different aspects in recent years (Refs. 1-6). It has been reported that weld metal is primarily influenced by the expitaxial grain growth at the fusion and heat-affected-zone interface. This growth proceeds across the weld deposit, creating long, oriented grains, which can have a detrimental influence on mechanical behavior. The epitaxial grains are the result of continual growth of the partially melted solid grains under the fusion line. Epitaxial growth requires a minimal undercooling to proceed, whereas nucleation of new weld metal grains requires that a significant free energy barrier be overcome. Consequently, substantial undercooling is necessary. This long columnar grain structure is not even broken up by multiple pass welds. The grains epitaxially grow from bead to bead across the complete deposit.

To achieve nucleation in the weld deposit and thus promote grain refinement, it is desirable to explore methods of reducing the free energy barrier or increasing the driving force (undercooling). Previously investigated methods include: 1) the use of grain refining additions to promote heterogeneous nucleation, 2) the stirring of the weld metal to promote dendrite fragmentation and thus new growth sites, and 3) the modification of the heat input to promote banding and other disrupted solidification behavior. One of these recent studies concludes that both the stray and equiaxed grains of the weld metal originate from heterogeneous nucleation; that such nucleation is favored by increased titanium content, and that constitutional undercooling plays only a secondary role in the microstructural development (Ref. 1). Other investigators (Refs. 2-9) describe the weld metal microstructure as being scarcely influenced by nucleation, but rather, as being totally controlled by the solidification rate. Misra, *et al.* (Ref. 10), has suggested that grain refinement must be considered a result of competitive nucleation and growth processes.

KEY WORDS

Grain Refinement
Aluminum Weld Metal
Ti/Zr Microadditions
Ti/Zr Grain Refiners
Solidification Rates
Nucleation Rate
Heterogenous Nucleation
Grain Refinement
Grain Refinement Model

The effects of welding speed and heat input on the weld metal macrostructure have been investigated for gas tungsten arc and electron beam welds on a variety of commercial aluminum alloys (Refs. 3, 4). It has been theoretically postulated that the nucleation of equiaxed grains depends on the extent of constitutional supercooling, as well as on the solidification temperature range. These conditions are in turn controlled by the material composition and the welding process parameters. Magnetic stirring has been shown (Ref. 2) to extend the range of welding conditions by producing a partially equiaxed structure and by increasing the fraction of equiaxed grains in the weld metal. Magnetic stirring is thought to lower the temperature gradient, thereby allowing nucleation and growth of aluminum grains further ahead of the columnar grains growing in from the solid-liquid interface (Ref. 2). To date, no experimental evidence has identified changes in constitutional undercooling arising from titanium additions to aluminum weld metal. However, the aluminum-titanium system provides a peritectic on the aluminum-rich end; and in the right compositions range, there is the possibility that fluctuations in the titanium content could provide substantial undercooling with the formation of the Al_3Ti intermetallic compound (Ref. 11).

A fundamental study of the nucleation mechanisms in Alloy 6061 weld metal has shown that heterogeneous nucleation is responsible for grain refinement (Refs. 5, 6). Dendrite fragmentation and grain detachment mechanisms are considered to be impossible for the 6061 aluminum weld metal during gas tungsten arc welding.

The purpose of this study was to investigate the change in solidification structure of 1100 series aluminum alloy welds as a function of titanium and zirconium additions for grain refinement. Relationships have been derived to show the influence of titanium and zirconium additions on solidifcation structure, grain

H. YUNJIA is with the Welding Research Division, Materials Science and Engineering Dept., Northwestern Polytechnical University of Xian, Shaanxi, China. R. H. FROST, D. L. OLSON and G. R. EDWARDS are with the Center for Welding and Joining Research, Colorado School of Mines, Golden, Colo.

Paper presented at the 67th Annual AWS Meeting, held April 13-18, 1986, in Atlanta, Ga.

refinement, and constitutional undercooling. Quantitative measurements of the influence of titanium and zirconium additions on grain size and orientation, grain growth velocity, and the time for nucleation of new grains have been made. These data have then been used to develop a model that relates process instabilities, constitutional undercooling, and heterogeneous nucleation to explain the role of titanium and zirconium in the grain refinement of the aluminum alloy weld metal.

Experimental Procedure

The base metal consisted of 1100 aluminum alloy plate with a thickness of 6.35 mm (0.25 in.). The titanium and zirconium grain refiners were added to the weld metal by inserting master alloy strips into a machined slot on the surface of the plate, and melting the alloy by three passes of a gas tungsten arc welding torch in the DCEP polarity. The master alloy strips were prepared by making titanium and zirconium foil additions to 1100 series aluminum. Ingots were cast in an inert atmosphere glove box, and the ingots were rolled to produce master alloy strips of the correct thickness.

The chemical compositions of the materials used are given in Table 1, and the welding parameters for the GTA welds are given in Table 2. The composition of the resulting weld deposit was determined by energy dispersive analysis on the scanning electron microscope.

Table 1—Chemical Analysis of Materials (wt-%)

Material	Si	Fe	Cu	Zn	Ti	Zr	Al
1100 alloy	0.06	0.5	0.1	0.001	–	–	Bal.
Titanium foil	0.34	–	–	–	99.66	–	–
Zirconium foil	0.82	–	0.4	–	–	98.72	0.06

Table 2—Gas Tungsten Arc Welding Parameters

Pass No.	Current (A)	Potential (V)	Travel Speed (mm/s)	Helium Flow (m^3/hr)
1	100	22	3.0	1.13
2	100	22	3.0	1.27
3	120	21	3.0	1.56

Experimental Results

The influence of zirconium additions on the solidification structure of the fusion zone is illustrated by the longitudinal micrographs in Fig. 1 for zirconium weld metal additions of 0.00, 0.05 and 0.23 wt-%. Figure 1A shows that without a grain refining zirconium addition, epitaxial growth led to a coarse columnar structure in which the large columnar grains had grown most of the way across the weld deposit. The addition of 0.05 wt-% zirconium to the weld metal refined the solidification microstructure as shown in Fig. 1B, and the addition of 0.23 wt-% zirconium, shown in Fig. 1C, refines the structure to an even greater extent. A comparison of these figures also shows that zirconium additions to the weld metal promoted extensive banding of the solidification structure.

Quantitative analysis of the longitudinal sections can be used to provide data on the extent of grain refinement provided by the zirconium additions. The measures

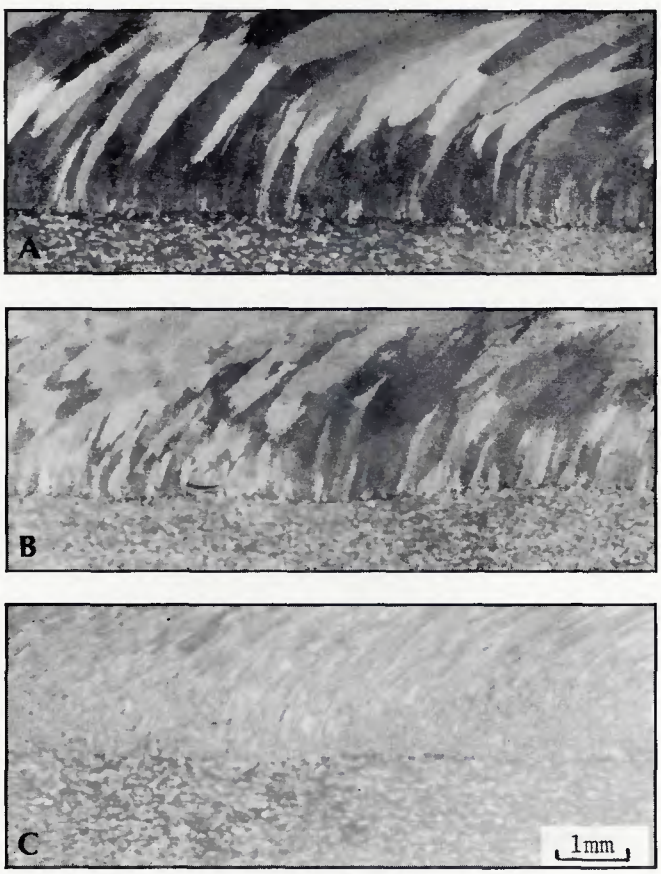

Fig. 1—Macrostructure from longitudinal sections as a function of increasing zirconium addition to 1100 aluminum weld metal. A—Zr = 0 wt-%, B—Zr = 0.05 wt-%, C—Zr = 0.23 wt-%

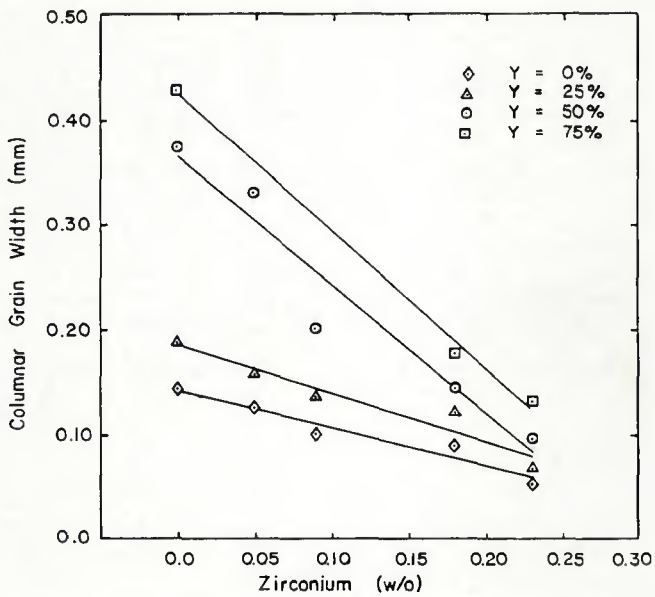

Fig. 2—Columnar grain width as a function of weld metal zirconium content in 1100 aluminum weld metal. The value Y is the fractional distance from the fusion line to the top surface of the weld

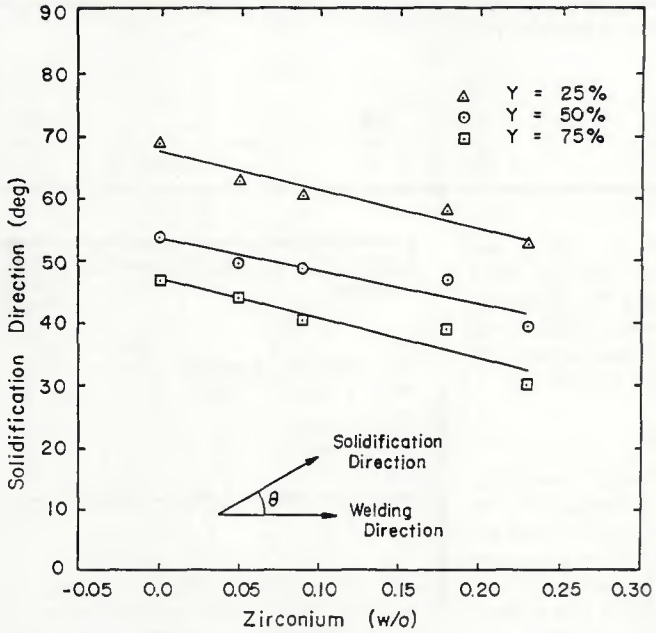

Fig. 3 – Solidification direction as a function of the zirconium content in 1100 aluminum weld metal. The value Y is the fractional distance from the fusion line to the top surface of the weld

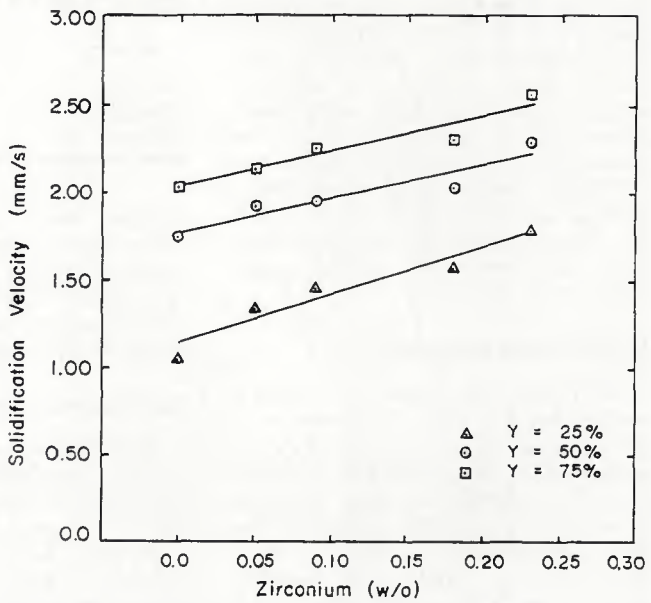

Fig. 4 – Solidification velocity as a function of the zirconium content in 1100 aluminum weld metal. The value Y is the fractional distance from the fusion line to the top surface of the weld

of structural refinement include the width of the columnar grains, the orientation angle of the grains with respect to the welding direction, the solidification velocity, and the average time for nucleation of new grains. Figure 2 shows the columnar grain width as a function of the zirconium concentration at the fusion line and at ¼, ½ and ¾ fractional distances (Y) from the fusion line to the top surface of the weld.

Without zirconium additions, small grains were obtained near the fusion line as a result of epitaxial growth, but very large columnar grains were obtained at the midpoint of the weld and beyond. Increasing zirconium additions refined the structure near the fusion line, but the greatest degree of grain refinement took place between the quarter weld thickness and the centerline of the weld. At a zirconium level of 0.23 wt-%, the columnar grain width at the midpoint of the weld was reduced from 0.375 to 0.094 mm. Both the width and length of the columnar grains were reduced as a function of increased zirconium additions, as shown in Figs. 1B and 1C.

Figure 3 shows the angle R between the growth direction of the columnar grains and the welding direction as a function of zirconium content and location in the weld. The angle between the growth and weld directions was reduced as the surface of the weld was approached, and nucleation events provided new grains whose growth direction was more closely aligned with the weld direction. Zirconium additions were observed to reduce the angle between the growth and weld directions at all locations in the weld. In the absence of zirconium, the columnar grains formed by epitaxial growth at the fusion line continued to grow toward the top surface of the weld.

The orientation of the columnar grains and the solidification velocity are related. More specifically, if one makes the approximation that the dendrites are aligned with the major axis of the grains, then as the growth direction approaches the welding direction, the solidification velocity increases. This relationship can

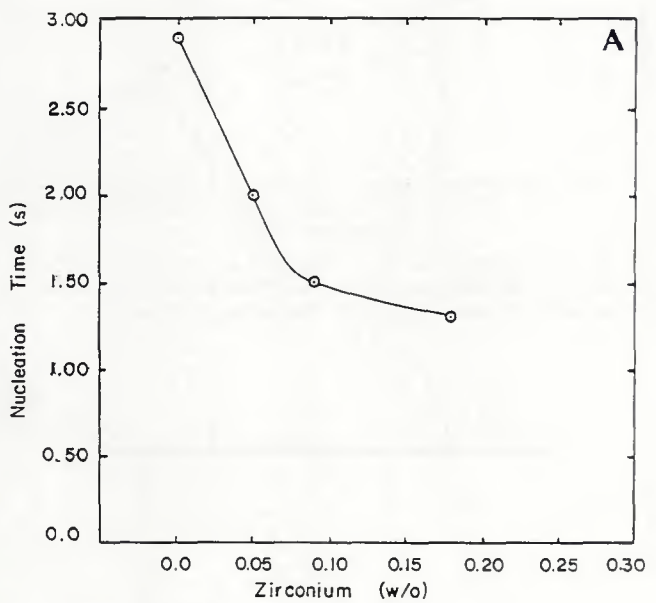

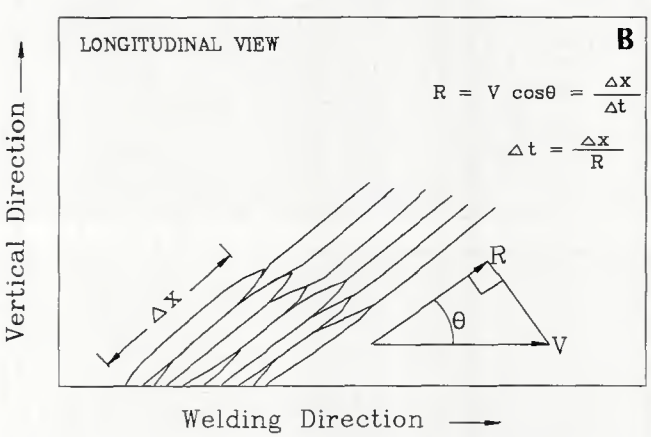

Fig. 5 – A – Nucleation time as a function of the zirconium content in 1100 aluminum weld metal; B – schematic illustration of nucleation time (Δt) determination

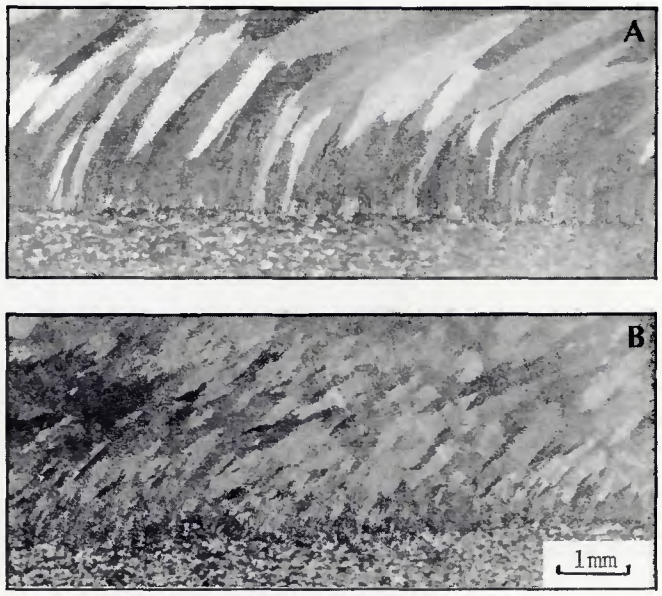

Fig. 6—Weld metal microstructure as a function of increasing titanium additions in 1100 aluminum weld metal. A—Ti = 0.0 wt-%; B—Ti = 0.13 wt-%

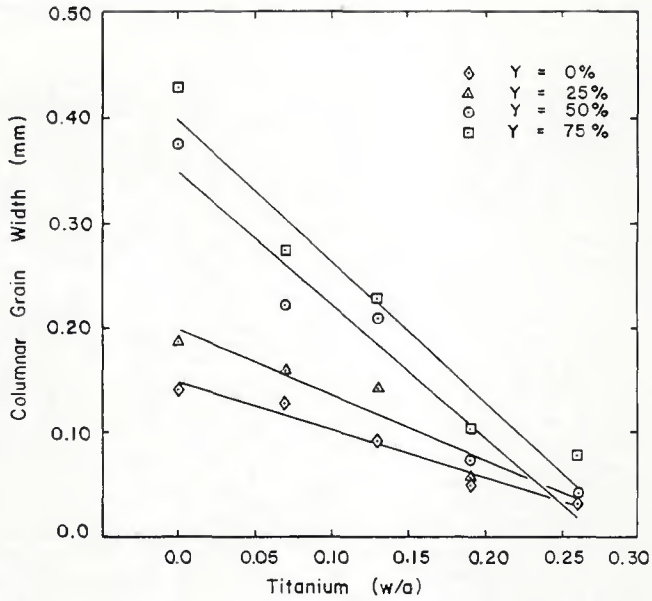

Fig. 7—Columnar grain width as a function of the titanium content in 1100 aluminum weld metal. The value Y is the fractional distance from the fusion line to the top surface of the weld

be expressed as follows:

$$R = V \cos\theta \quad (1)$$

where R is the solidification velocity and V is the welding velocity. Figure 4 shows the increase in solidification velocity with increasing zirconium additions at the ¼, ½, and ¾ weld thickness positions. The overall influence of the zirconium additions was to cause a decrease in the time available for the nucleation of new grains. Figure 5A shows the nucleation time of new grains and illustrates the decrease in nucleation time with increasing zirconium content. The nucleation times shown on this plot were calculated by dividing the distance between nucleation events along the columnar grain by the solidification velocity, as shown in Fig. 5B. Notice that the solidification rate and nucleation rate were both increased by the grain refiner. This suggests that a thorough understanding of grain refinement requires consideration of nucleation and growth as competitive processes.

The influence of titanium additions on weld metal microstructure was similar to that of zirconium, as shown in Fig. 6. Figures 6A and 6B are photomacrographs taken along a longitudinal section of a weld produced without titanium and with a 0.13 wt-% titanium addition, respectively. The titanium refines the solidification structure. Figures 7 to 10 show the columnar grain width, the orientation angle for the columnar grains, the solidification velocity, and the nucleation time as functions of the titanium content of the weld metal. Comparisons of these data with Figs. 2–5 show that these results were quite similar in features and magnitude to those obtained by making zirconium additions to the weld metal. It appears that zirconium and titanium additions based on wt-% are equivalent in their grain refining ability.

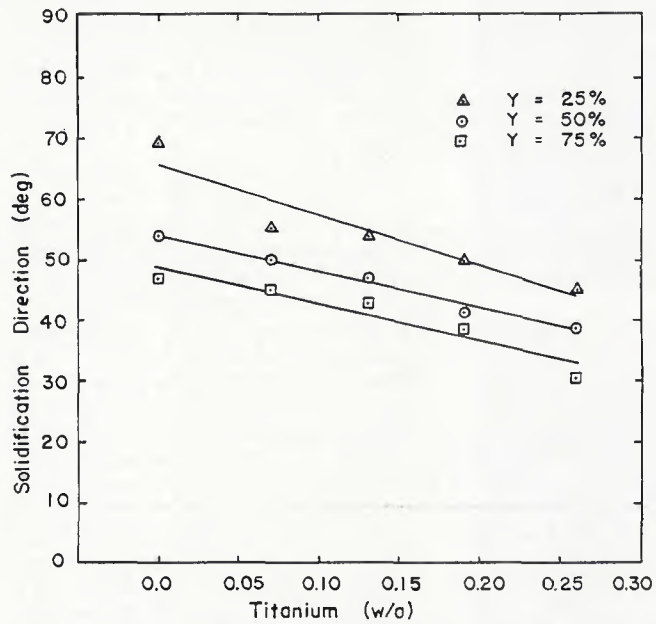

Fig. 8—Solidification direction as a function of the titanium content in 1100 aluminum weld metal. The value Y is the fractional distance from the fusion line to the top surface of the weld

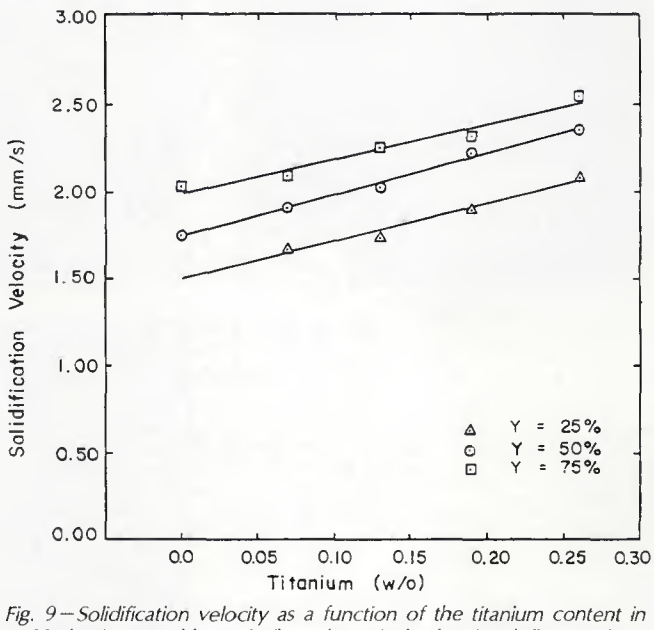

Fig. 9—Solidification velocity as a function of the titanium content in 1100 aluminum weld metal. The value Y is the fractional distance from the fusion line to the top surface of the weld

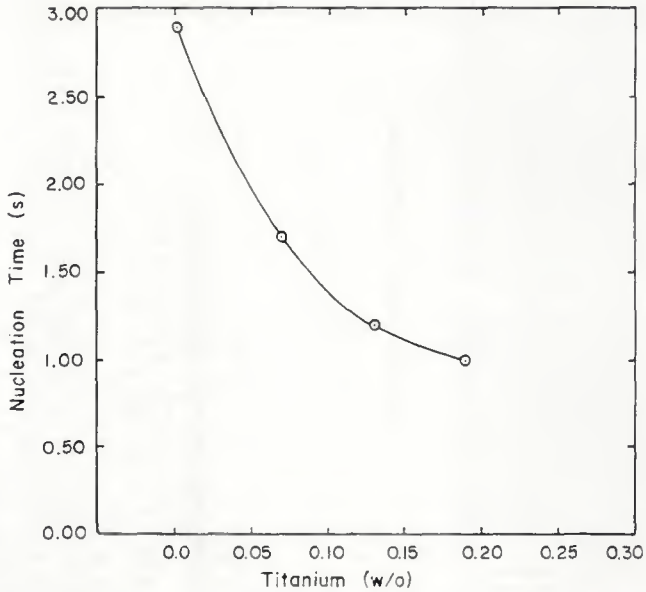

Fig. 10—Nucleation time as a function of the titanium content in 1100 aluminum weld metal

Fig. 11—Solidification structure of 1100 aluminum weld metal with: A—0.07 wt-% titanium addition; B—0.19 wt-% titanium addition; C—0.19 wt-% titanium addition; D—0.26 wt-% titanium addition; E—0.31 wt-% titanium addition

In addition to the promotion of grain refinement, additions of titanium to aluminum alloy welds promote a shift in the solidification structure from cells at high ratios of the thermal gradient to solidification velocity (G/R) toward equiaxed dendrites at low G/R ratios. Figure 11 shows by means of scanning electron micrographs of deep-etched weld metal the change in solidification structure from: A) cellular, B) cellular dendrites, to C) dendrites, to D) columnar dendrites, and finally to E) equiaxed dendrites when increasing amounts of titanium are added to the 1100 aluminum. Classification of the solidification mode as a function of the titanium concentration and the location in the weld (Y) is quantified in Fig. 12. These results emphasize that the structure progresses from cellular toward equiaxed dendrites with increasing titanium or with distance from the fusion line. Not only were titanium additions found to alter the character of the solidification substructure, but they also were found to refine the substructure, as shown in Fig. 13. Here, the cell spacing is shown to decrease with increasing titanium content.

A commonly accepted view of solidification kinetics (Ref. 12) holds that the solidification mode can be classified by regions in a plot of percent solute versus the ratio $G/(R)^{1/2}$, as shown schematically in Fig. 14. The data for the titanium welds of this study are classified in Fig. 15 according to the scheme suggested by Fig. 14. The thermal gradients were calculated using the equation of Katoh, *et al.* (Ref. 13), and the welding parameters given in Table 2. The results indicate that, in spite of the severe thermal gradients and rapid solidification rates present, these titanium-enriched 1100 aluminum weld metals can be analyzed in terms classically reserved for solidification of castings.

Figures 16A and 16B are scanning electron micrographs of aluminum-titanium welds that show banding and the nucleation of new aluminum dendrites immediately after the band. Figures 17A and 17B are SEM micrographs that show a columnar dendrite nucleated on a $TiAl_3$ particle and a micrograph of the same particle at higher magnification. Figures 18A and 18B are similar SEM micrographs that illustrate heterogeneous nucleation of an equiaxed dendrite on a $TiAl_3$ particle. Table 3 shows the energy dispersive analysis of the $TiAl_3$ particles shown in Figs. 17 and 18. Analysis of these micrographs suggests that one of the possible nucleation mechanisms providing grain refinement is associated with particles of the $TiAl_3$ phase.

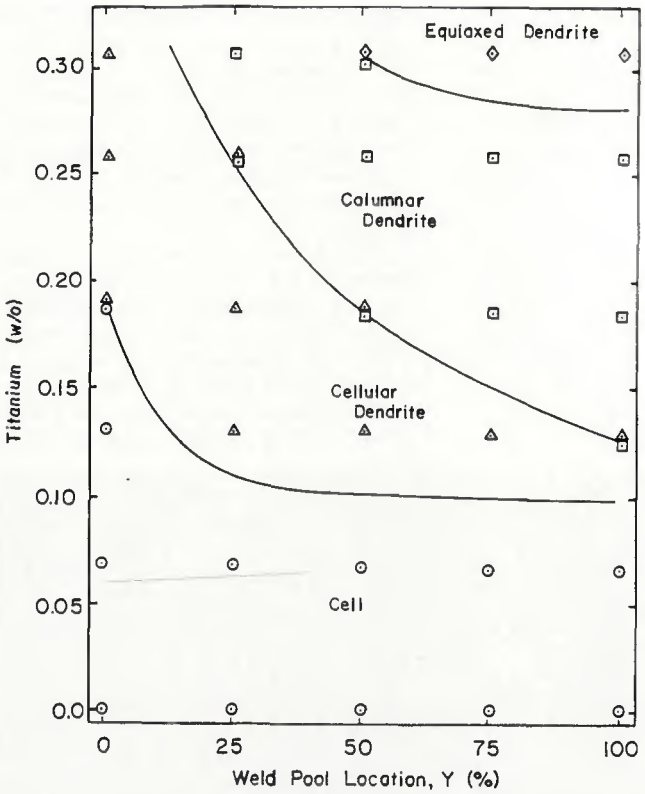

Fig. 12—Solidification mode as a function of weld pool location and titanium content in 1100 aluminum weld metal

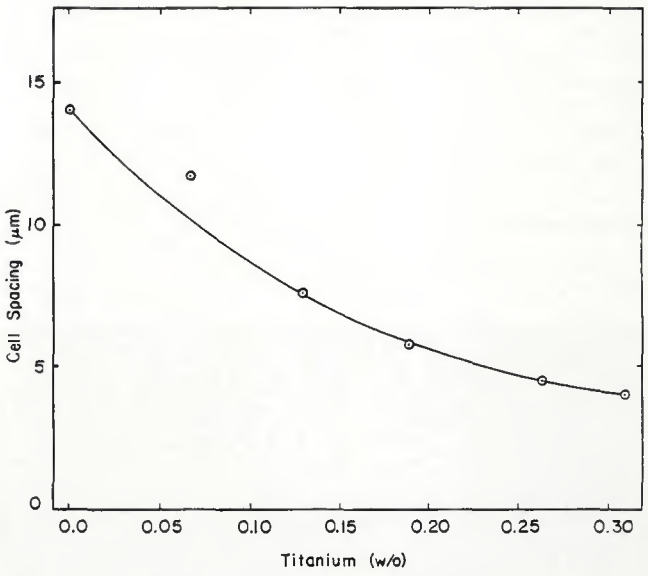

Fig. 13—Cell spacing at the fusion line for the epitaxial growth as a function of the titanium content in 1100 aluminum weld metal

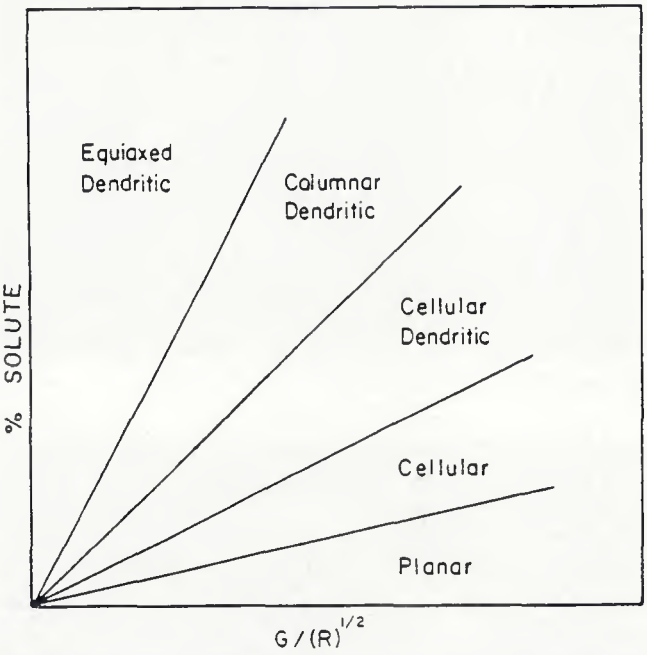

Fig. 14—Schematic illustration of the influence of the temperature gradient (G), growth rate (R) and solute content on the solidification mode

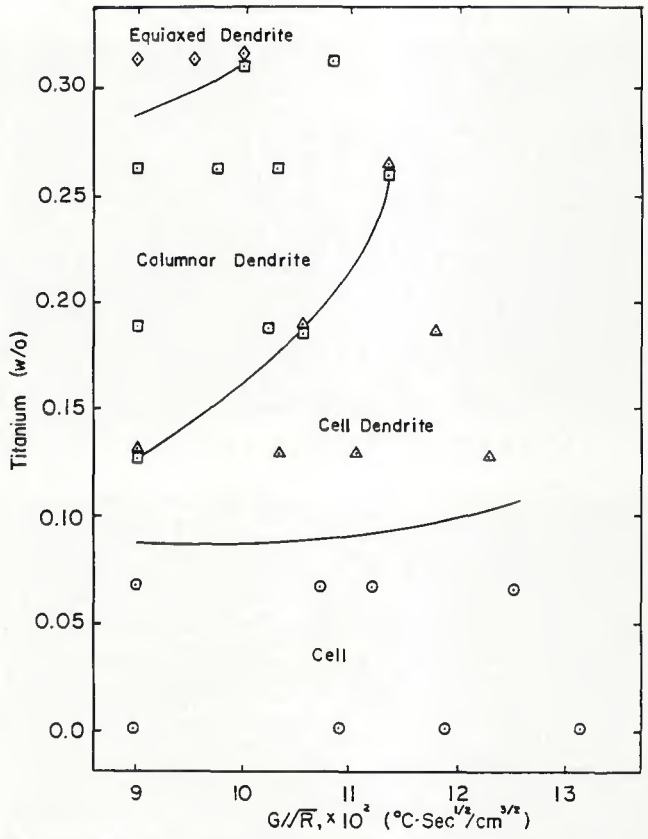

Fig. 15—Influence of temperature gradient (G), growth rate (R) and titanium content on the solidification mode in 1100 aluminum weld metal

Discussion

Several possible explanations are available for the weld metal microstructural refinement caused by zirconium and titanium additions. The following discussion will consider the evidence for the possibilities as provided by optical metallography, scanning electron metallography, and energy dispersive spectrum (EDS) analysis of compositions on a microscopic scale.

Crystal Fragmentation

The weld metal microstructures were examined by scanning electron microscopy for dendrite fragmentation. The surfaces of welds containing titanium were deeply etched using a solution containing 6 mL HF, 25 mL HNO_3, and 78 mL HCl. The surfaces were not subjected to deformation, grinding or polishing in order to avoid the mechanical formation of dendrite fragments. After deep etching, the specimens were examined in the scanning electron microscope, and a variety of dendrite fragments were found. Figures 19 to 21 show SEM micrographs of dendrite fragments on the surface of a weld containing 0.265 wt-% titanium. The dendrite fragments in Figs. 19 and 20 were clearly present during the solidification process, but they do not appear to have grown so as to control the weld metal grain structure. Figure 21 shows some evidence that growth in the direction of the thermal gradient has caused the dendrite fragments to bend; however, fragments were few in number, and no correlation between the number of fragments and the final grain size could be made.

The phenomenon of dendrite fragmentation is well known in the solidification of castings and ingots (Ref. 14). Based on the microstructures observed for the welds in the present study, however, it is doubtful that a sufficient number of dendrite fragments survived or continued growth for a dendrite fragmentation

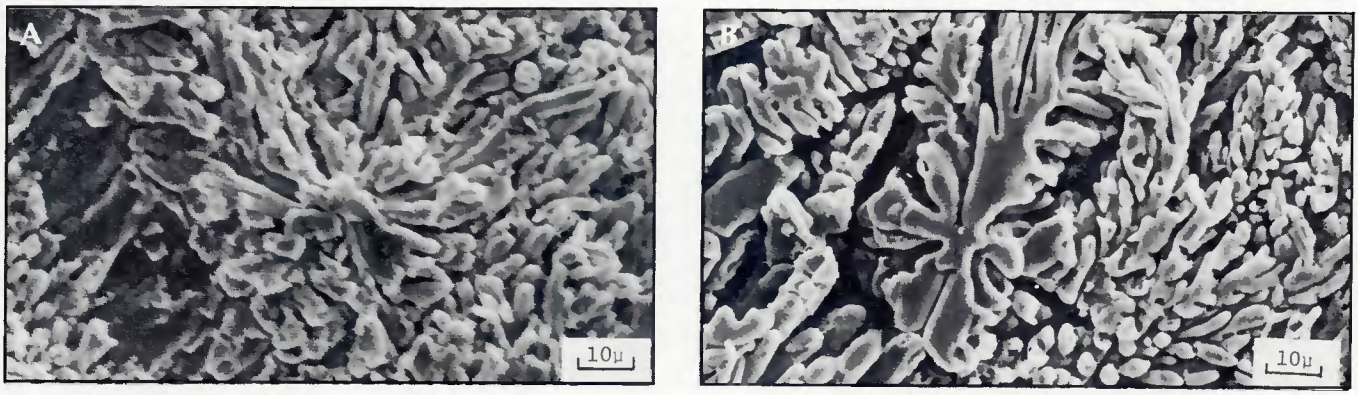

Fig. 16—Solidification substructure at solute bending in 1100 aluminum weld metal with 0.26 wt-% titanium. A—Surface section; B—longitudinal section

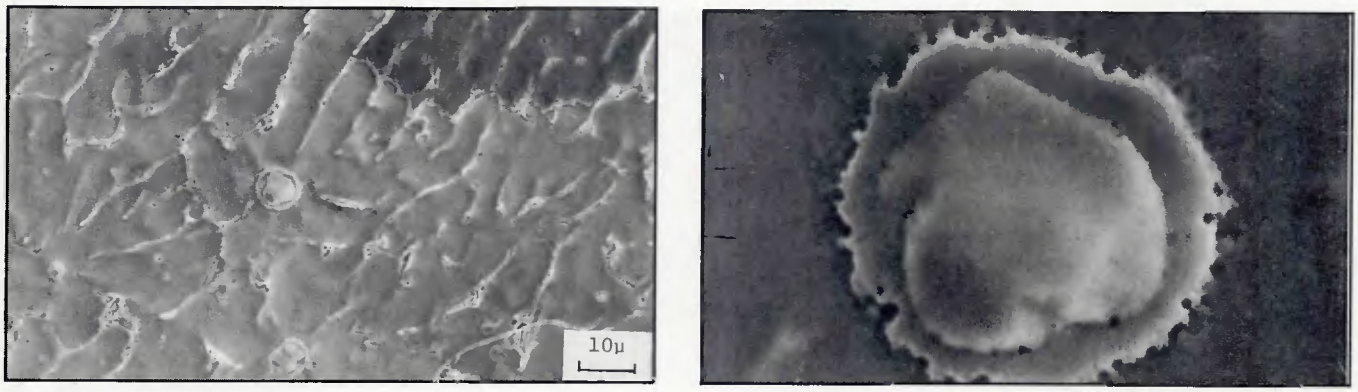

Fig. 17—Columar dendrite originating from a $TiAl_3$ particle in 1100 aluminum weld metal with 0.31 wt-% titanium

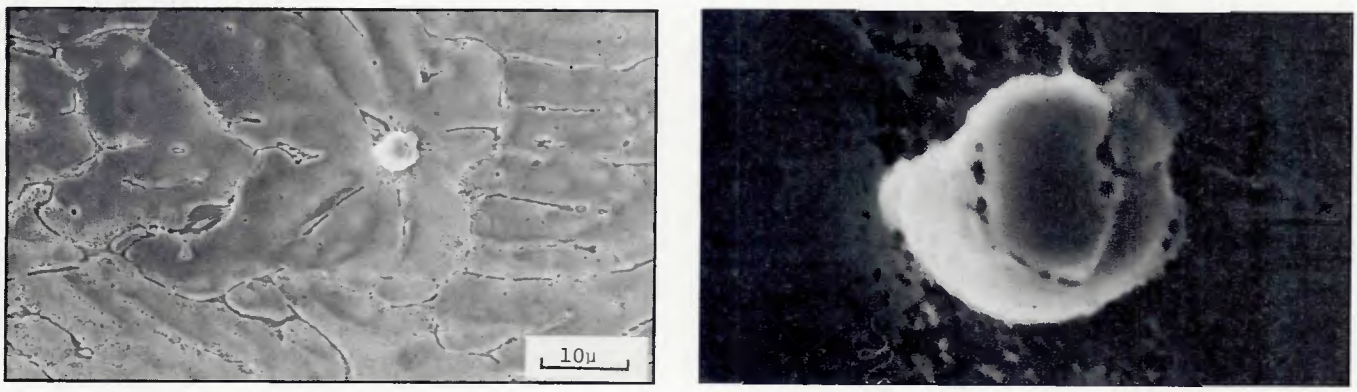

Fig. 18—Equiaxed dendrite originating from a $TiAl_3$ particle in titanium microalloyed 1100 aluminum weld metal

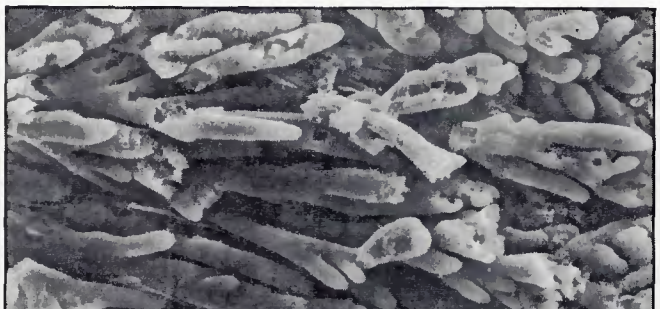

Fig. 19—Dendrite fragmentation on the surface of a weld with 0.26 wt-% titanium (near to the center of the weld)

Fig. 20—Dendrite fragmentation on the surface of a weld with 0.26 wt-% titanium (at a solute band) in 1100 aluminum weld metal

model to control refinement of the solidification structure. Therefore, the increase in grain refinement with increasing titanium or zirconium additions suggests that titanium and zirconium promoted heterogeneous nucleation of new grains.

Table 3—EDS Data for 1100 Aluminum Weld Metal with 0.31 wt-% Titanium

Number	% Al	% Ti	% Si	% Fe	Location Analyzed
1	64.48	33.97	0	0	Center in Fig. 17
2	60.47	31.64	0	6.14	Center in Fig. 18

Heterogeneous Nucleation of New Grains

The fact that additions of titanium or zirconium promote refinement of cellular or dendritic weld metal structures implies their involvement in the nucleation process. Classical nucleation and growth theories may be modified and applied to the weld pool (Refs. 10, 15) by introducing two competing times. Consider the time, t_n, to nucleate one grain:

$$t_n = \frac{C_1}{V} \exp\left[\frac{+16\sigma^3 T_m^2 V_s^2 f(\theta)}{3\Delta H^2 \Delta T^2 kT}\right] \quad (2)$$

where ΔH is the degree of undercooling; T_m is the melting temperature; k is Boltzmann's constant; V_s is the atomic volume of solid; V is a volume element in the weld pool that can be assumed to be a unit volume; $f(\theta)$ is the function of contact angle, and C_1 is a constant.

Secondly, consider the time, t_g, for an epitaxial grain to grow across the total depth of a weld bead:

$$t_g = \frac{X_o}{K_s \Delta T} \quad (3)$$

where X_o is the bead depth and K_s is the solidification rate constant.

Figure 22 shows a schematic illustration of the effects of the nucleation and growth rates on refinement of the solidification structure (Ref. 10). The plot shows the time for growth of the columnar grain across the weld bead (t_g) and the average time for a nucleation event to occur (t_n) plotted as a function of the thermal undercooling at the solidification interface (ΔT). At undercoolings (ΔT_w) less than the critical undercooling (ΔT_C), the columnar grain grows across the weld before nucleation occurs, and a coarse solidification structure results. At undercoolings greater than the critical undercooling (ΔT_c), nucleation occurs before the columnar grain can grow across the weld, and the result is the refinement of the weld solidification structure. If this mechanism is valid, then titanium or zirconium additions may be assumed to alter the critical undercooling, thereby reducing the average time for heterogeneous nucleation more than they decrease the time required for a grain to grow across the weld bead.

The mechanism by which titanium or zirconium influence the nucleation of new grains can involve constitutional undercooling ahead of the solid/liquid interface, and the development of macrosegregation in the form of banding caused by process transients and instabilities in the heat flow. Consider the binary phase diagrams for simple eutectic and peritectic systems. For any eutectic system, the equilibrium partition ratio is less than one, and the composition of any hypoeutectic solid is lower than the liquid composition at the solid/liquid interface. The lack of solid diffusion leaves a depleted solute concentration of the first solid to form (dendrite centerline). In a peritectic system, on the other hand, the equilibrium partition ratio greater than 1.0 causes solute enrichment at the dendrite centerline and solute depletion in the last interdendritic liquid to solidify.

The aluminum-titanium and aluminum-zirconium binary phase diagrams both contain peritectic invariant reactions. The expanded aluminum-rich end of the aluminum-titanium phase diagram is shown in Fig. 23 (Ref. 11). The peritectic temperature is 938 K. At this temperature, the liquid (0.15 wt-% Ti) and the intermetallic compound $TiAl_3$ react to form an aluminum solid solution with a composition of 1.08 wt-% titanium. An alloy with less than 0.15 wt-% titanium will solidify to form titanium-enriched aluminum dendrites, and the titanium concentration in the interdendritic liquid will decrease with increasing depth in the mushy zone. An alloy with greater than 0.15 wt-% titanium will form the $TiAl_3$ primary phase

Fig. 21—Crystal distortion and fragmentation in weld metal

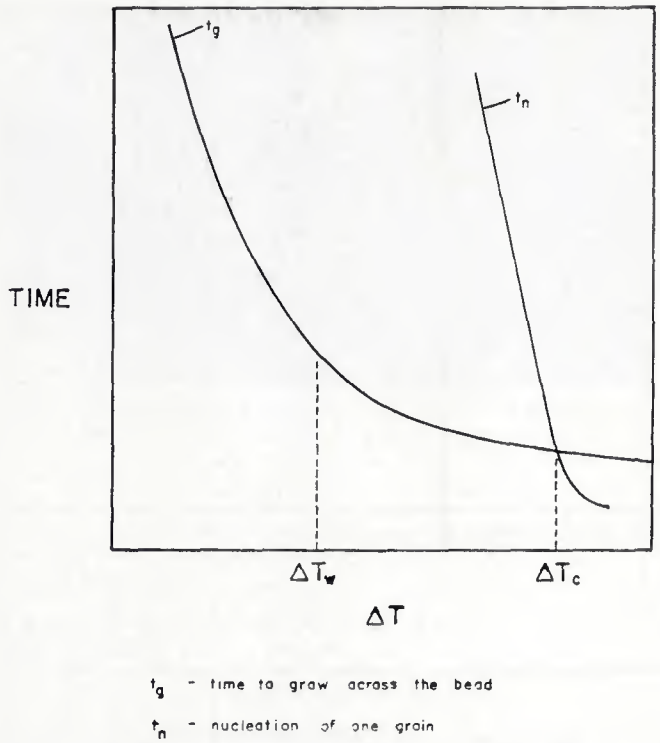

Fig. 22 – Time to nucleate a new grain and time to grow across the weld bead as a function of undercooling during weld metal solidification

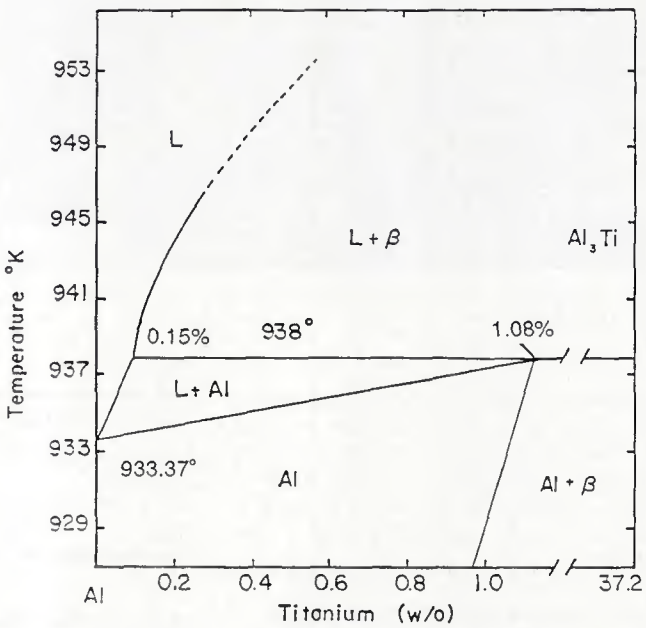

Fig. 23 – Expanded aluminum-rich end of the aluminum-titanium binary phase diagram (Ref. 11)

above the peritectic temperature (Ref. 16). Under equilibrium conditions, the $TiAl_3$ will react with the liquid at the peritectic temperature to form the aluminum phase. However, under the conditions expected for weld solidification, the $TiAl_3$ particles probably act as nucleation sites for the aluminum phase, and become surrounded by aluminum such that the equilibrium peritectic reaction is prevented. It is known that $TiAl_3$ is a potent nucleant for aluminum grain refining (Ref. 17). The aluminum alloys investigated in this study have titanium additions varying from 0.07 to 0.31 wt-%. Impurities such as iron and silicon should decrease the titanium concentration required for the formation of $TiAl_3$ from the melt. With the addition of ternary or quaternary components to the system, titanium concentrations as low as 0.07 wt-% may produce the few $TiAl_3$ particles necessary for nucleation of new aluminum grains, thereby accomplishing grain refinement of the weld metal.

The nucleation events in the present experiments occurred in bands that correlated with the banding type macrosegregation caused by thermal instabilities in the welding process (Refs. 18–20). This suggests that the thermal instabilities cause compositional fluctuations in the liquid within the peritectic region. Figure 23 illustrates that a small compositional fluctuation within the peritectic region can cause a very substantial undercooling. This leads to the nucleation of $TiAl_3$ particles, and these particles cause the nucleation of new aluminum dendrites.

Conclusions

1) Additions of zirconium up to 0.23 wt-% and of titanium up to 0.26 wt-% have been shown to siginficantly refine the grain size of 1100 aluminum gas tungsten arc weld metal.

2) Zirconium and titanium additions to 1100 aluminum GTA weld metal increase the solidification velocity and decrease the grain nucleation time.

3) While dendrite fragmentation was observed near the free surface of titanium- or zirconium-enriched 1100 aluminum welds, insufficient evidence of fragmentation was found to account for the grain refinement observed.

4) Dendrite nucleation was found to be correlated with solute banding and with $TiAl_3$ particles in titanium-enriched 1100 aluminum weld metal. Consequently, a qualitative model was proposed to explain grain refinement. This model suggests that enhanced constitutional supercooling, coupled with compositional banding, leads to nonequilibrium precipitation of $TiAl_3$ nucleants.

5) Solidification modes have been classified for titanium-enriched 1100 aluminum GTA weld metals, and the modes have been shown to be consistent with commonly accepted concepts of solidification theory.

Acknowledgments

The authors appreciate and acknowledge the research support of the U.S. Army Research Office and the living expense support for Prof. He Yunjia from the Northwestern Polytechnical University of Xian, China.

References

1. Ganaha, G., Pearce, B. P., and Kerr, H. W. 1980. Grain structure in aluminum alloy GTA welds. *Met. Trans.* 11A (8):1351–1359.

2. Pearce, B. P., and Kerr, H. W. 1981. Grain refinement in magnetically stirred GTA welds of aluminum alloys. *Met. Trans.* 12B (9):479–486.

3. Arata, Y., Matsuda, F., Mukae, S., and Katoh, M. 1973. Effect of weld solidification mode on tensile properties of aluminum weld metal. *JWRI* 2(2).

4. Arata, Y., Matsuda, F., and Nakata, K. 1976. Effect of solidification rate on solidification structure in weld metal. *Trans. JWRI* 5(1):47–52.

5. Kou, S., and Le, Y. 1985. *Nucleation Mechanisms and Grain Refining of Weld Metal – A Fundamental Study*. University of Wisconsin, Madison, Wis.

6. Kou, S., and Sun, D. K. 1985. Fluid flow and weld penetration in stationary arc welds. *Met. Trans.* 16A(2):203–213.

7. Savage, W. F., Lundin, C. D., and Aronson, A. H. 1965. Weld Metal solidification mechanics. *Welding Journal* 44(4):175-s to 181-s.

8. Savage, W. F., and Aronson, A. H. 1966. Preferred orientation in the weld fusion zone. *Welding Journal* 45(2):85-s to 89-s.

9. Loper, C. R., and Gregory, G. T. 1974. Microstructural aspects of weld metal solidification in large grain aluminum. *Welding Journal* 53(3):126-s to 133-s.

10. Misra, M. S., Olson, D. L., and Edwards, G. R. 1982. The influence of process parameters and specific additions on epitaxial growth in multipass Ti-6Al-4V welds. Proc., AIME Con. *Grain Refinement in Castings and Welds*, St. Louis, Mo.

11. *Metals Handbook*, Vol. 8, 8th Edition, 1973. ASM International, Metals Park, Ohio.

12. Flemings, M. C. 1974. *Solidification Processing*, McGraw-Hill, New York, N.Y.

13. Katoh, M., Matsuda, F., and Senda, T. 1972. Solidification mode in aluminum weld metal. *Trans. J.W.S.* 3:69.

14. Davies, G. J., and Garland, J. G. 1975. Solidification structure and properties of fusion welds. *Int. Met. Rev.* 20:83-106.

15. Nordin, M. C. 1985. The effects of yttrium on grain refinement and cracking susceptibility in Ti-6Al-2N.b.-1Ta-0.8Mo weld metal. Thesis T-3036, Colorado School of Mines, Golden, Colo.

16. Mondolfo, L. F. 1976. *Aluminum Alloys—Structure and Properties*. Butterworths, London, p. 386.

17. Kerr, H. W., Cisse, J., and Bolling, G. F. 1974. On equilibrium and non-equilibrium peritectic transformations. *Acta. Met.* 22(6):677-686.

18. Flemings, M. C., and Nereo, G. E. 1967. Macrosegregation: Part I. *Trans. Soc. of AIME* 239(9):1449-1461.

19. Flemings, M. C., Mehrabian, R., and Nereo, G. E. 1968. Macrosegregation: Part II. *Trans. Met. Soc. of AIME* 242(11):41-49.

20. D'Annessa, A. T. 1970. Sources and effects of growth rate fluctuations during weld metal solidification. *Welding Journal* 49(2):41-s to 45-s.